Optimization of the key position parameters for tractor steering wheel based on a driver's arm muscle load analysis

Hongmei Xu[1,2], Hao Yang[1,2], Yujun Shang[1,2], Yinpei Zhang[1,2], Zhangfen Liu[1,2], Qichao Wang[1,2], Guozhong Zhang[1,2*]

(1. *College of Engineering, Huazhong Agricultural University, Wuhan 430070, China*;
2. *Key Laboratory of Agricultural Equipment in Mid-lower Reaches of the Yangtze River, Ministry of Agriculture and Rural Affairs, Huazhong Agricultural University, Wuhan 430070, China*)

Abstract: Steering wheel is the most frequently used manual device in tractors, whose position directly affects the handling comfort of the driver and fatigue degree of the arm muscles. In this study, the biomechanical modelling software AnyBody was used for an inverse kinetics analysis of the rotation process of tractor steering wheel, calculate the muscle activation degree of the driver's arm and compare it with the calculated results of surface EMG tests to verify the reliability of the biomechanical model. Based on the biomechanical model, the effects of three position parameters (steering wheel inclination, front-back distance, and upper-lower height) on the activation degree of the driver's arm muscles were evaluated. The results demonstrated that steering wheel inclination has the most significant effect on the degree of muscle activation, followed by the upper-lower height and then front-back distance. Considering the interaction among factors, a regression orthogonal test was designed, and the test results revealed that the minimum muscle activation (1.2887) can be obtained with the steering wheel inclination of 31°, front-back distance of 431 mm and upper-lower height of 375 mm. The findings can provide a reference for optimizing the structure and position parameters of tractor steering wheels.

Keywords: tractor, steering wheel, driver's arm, biomechanical characteristics, position parameter optimization
DOI: 10.25165/j.ijabe.20231605.7996

Citation: Xu H M, Yang H, Shang Y J, Zhang Y P, Liu Z F, Wang Q C, et al. Optimization of the key position parameters for tractor steering wheel based on a driver's arm muscle load analysis. Int J Agric & Biol Eng, 2023; 16(5): 236–247.

1 Introduction

Tractors are widely used in nearly all aspects of agricultural production as a key source of power. Frequent rotation of the steering wheel during the driving process tends to cause the accumulation of arm muscle fatigue, which not only reduces the efficiency and comfort of the operation, but also threatens the personal safety of the driver. Steering wheel is the most frequently used manual control device in the tractor. Its space position directly affects the operation comfort and the arm muscle fatigue degree of the driver. Therefore, optimization of the position parameters of steering wheel can effectively improve the operation comfort of tractor drivers[1].

In recent years, increasing research has been carried out on the optimization of position parameters for handling devices in the tractor cab. For example, Yang et al.[2] built a test system and biomechanical model for the driver-clutch pedal interaction characteristics in tractors to analyze the human-machine interaction characteristics, as well as studied the influence of clutch pedal resistance and pedal layout on the driver's handling comfort based on the simulation results. Musale et al.[3] designed an adjustable clutch pedal assembly, analyzed the ergonomic position of the 5th and 95th percentile drivers, and improved handling comfort by adjusting the position parameters of the accelerator, brake pedal and clutch pedal. Feyzi et al.[4] calculated the minimum permissible driving force of the pedal by measuring the muscular force of the foot on the pedal and pushing/pulling of the joystick, and obtained an ergonomically optimal design based on the physical characteristics, which could reduce the fatigue of the tractor driver to certain extent. Qin et al.[5] established a comprehensive evaluation index system for tractor pedal comfort based on sitting and handling comfort, and determined the comfort range and optimum levels of pedal position parameters through single-factor test; on this basis, they analyzed the mechanism for the influence of position parameters on pedal comfort, and optimized and verified the pedal position parameters. Jin et al.[6] successfully improved the comfort and efficiency of the joystick by optimizing its position parameters based on the theoretical ergonomics. Zhang et al.[7] established a tractor driver-cab coupled biomechanical model, and analyzed the fatigue level of the driver's lower limbs by simulating the dynamic process of pedal manipulation, which provided a reference for the optimal layout of cab manipulation devices. Jiang[8] established a comprehensive evaluation system for steering wheel comfort based on sitting and handling comfort, and optimized the position parameters through single-factor test and orthogonal test. In summary, plenty of research has been carried out on the

Received date: 2022-10-24 **Accepted date:** 2023-03-30
Biographies: Hongmei Xu, PhD, Associate Professor, research interest: vibration comfort of agricultural machinery, Email: xhm790912@163.com; **Hao Yang**, MS candidate, research interest: vibration comfort of agricultural machinery, Email: 1371710254@qq.com; **Yujun Shang**, MS candidate, research interest: vibration comfort of agricultural machinery, Email: 825675910@qq.com; **Yinpei Zhang**, MS candidate, research interest: vibration comfort of agricultural machinery, Email: 1066732953@qq.com; **Zhangfen Liu**, MS candidate, research interest: vibration comfort of agricultural machinery, Email: 1021465716@qq.com; **Qichao Wang**, MS candidate, research interest: vibration comfort of agricultural machinery, Email: 2503548861@qq.com.
***Corresponding author: Guozhong Zhang**, PhD, Professor, research interest: Agricultural mechanization and automation, College of Engineering, Huazhong Agricultural University, No1, Shizishan Street, Hongshan District, Wuhan 430070, China. Tel: +86-18672783365, Email: zhanggz@mail.hzau.edu.cn.

optimization of position parameters of the handling devices in the tractor cab, which has generated fruitful results. However, the optimization of steering wheel position parameters is mainly carried out in terms of torsional moment and arm extension difficulty, while there has been little research with the aim to reduce the fatigue of the driver's arm.

Therefore, this study used the biomechanical modeling software AnyBody to establish a biomechanical model for the tractor driver, based on which the steering wheel rotation was simulated. An inverse dynamics analysis was performed to calculate the activation degree of the main muscles of the driver's arm, and analyze its changing trend during anticlockwise rotation of the steering wheel. Then, a single factor analysis and a response surface analysis were used to simulate the combination of different position parameters of the steering wheel. By taking the muscle activation degree as the index, the position parameters of the tractor steering wheel were simulated and optimized to determine the optimal combination. The findings can provide reference for the optimization of the structure and position parameters of tractor steering wheel.

2 Methods

2.1 Establishment of biomechanical coupling model for tractor driver and steering wheel

AnyBody is a simulation analysis software combining both ergonomics and biomechanics, and mainly calculates the joint force and muscle load of human body through inverse dynamics analysis, which can analyze the load state and fatigue degree of the human body from the perspective of biomechanics. As a biomechanical modeling software with an independent scripting language, AnyBody has the advantages of convenience, high speed and clarity in model processing, simulation analysis, chart display and data output[9]. To build a biomechanical model for a tractor driver based on AnyBody, the musculoskeletal model in the library of AnyBody must be scaled to obtain a human musculoskeletal model that matches with the actual study; secondly, the posture of the human musculoskeletal model must be adjusted to be consistent with the actual driving posture; finally, an external environment model related to the human musculoskeletal model should be established, and the human musculoskeletal model should be coupled with the external environment model.

2.1.1 Establishment of biomechanical model for driver's musculoskeletal system

1) Construction of the basic model for the driver

The musculoskeletal model in AnyBody was derived from the human musculoskeletal model library established by the Aalborg University in Denmark, which has different functions to scale the model to the size required by the user Liu et al.[10] In this study, scaling of the musculoskeletal model was performed based on external body measurements. AnyBody specifies the location of skeletal markers and the body movements during external measurements (Figure 1), where the subject's upper body is measured for head length, big arm length, small arm length, hand length and hand width, and the lower body is measured for thigh length, calf length and foot length.

In this study, three subjects at the 50th percentile were selected for measurement of their external body dimensions. The subjects were asked to stand and perform the prescribed movements, and the main parameters of their upper and lower body dimensions were measured. The average of the dimensions from the three subjects was calculated, and the results are listed in Table 1.

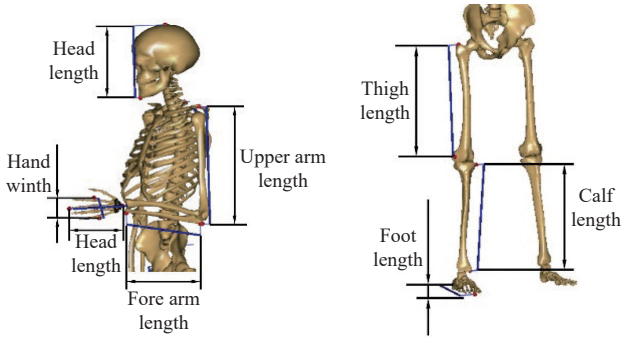

Figure 1 Marker position and human action

Table 1 External dimensions of subjects in the 50th percentile (cm)

Head length	Upper arm length	Fore arm length	Hand length	Hand width	Thigh length	Calf length	Foot length
24	31	24.5	19.5	9	44	39	25.5

Based on the measured external dimensions of the driver's body, the human musculoskeletal model was scaled in AnyBody to obtain the realistic musculoskeletal model of the driver at each percentile of the study.

2) Posture adjustment of the driver musculoskeletal model

The basic model provided by AnyBody is in a standing position, and therefore the model needs to be adapted to the actual driving position. In addition, for the subsequent coupling of the human body model with the external environment model, it is necessary to determine the horizontal and vertical distances from the steering wheel midpoint (*W* point) to the hip point (H Point), which is the reference point for the cab layout in ergonomics[11]. Measurements of the angle and distance of each joint are shown in Figure 2.

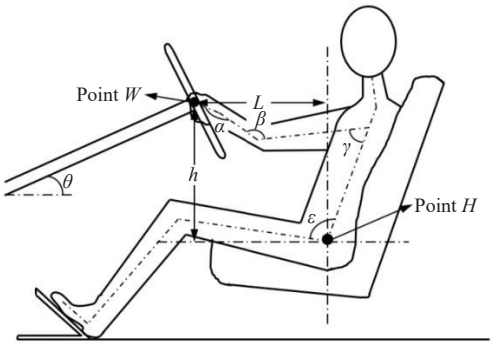

Figure 2 Schematic diagram for the measurement of driver sitting posture

According to the driving posture measurement schematic diagram, the angle of each joint and the associated distance are measured with the driver sitting in the tractor at the driving posture. The specific parameters are listed in Table 2.

Table 2 Joint angle and associated distance under driving posture of the 50th percentile driver

Symbol	Meaning	Value
L/cm	Horizontal distance from W to *H* point	45.54
h/cm	Vertical distance from W to *H* point	33.65
α/(°)	Angle between thigh and trunk	109.31
β/(°)	Angle between arm and trunk	61.15
γ/(°)	Angle between the small arm and big arm	161.09
ε/(°)	Angle between hand and arm	165.30
θ/(°)	Steering wheel inclination angle	40.00

Based on the data in Table 2, the corresponding joint angles in the human musculoskeletal model were adjusted to obtain a musculoskeletal model for the driving posture as shown in Figure 3.

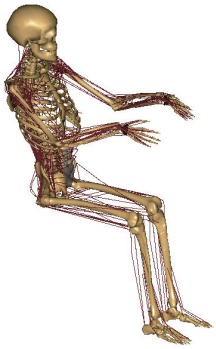

Figure 3 Musculoskeletal model for the driving posture

2.1.2 Construction of steering wheel manipulation environment model

Once the musculoskeletal model of the driving posture is created, it is necessary to establish an external environment model and couple it with the musculoskeletal model. The contact between the driver and the cab mainly includes the contacts between the hands and the steering wheel, between the lower back and the backrest, between the hips and the cushion and between the feet and the floor[12,13]. In order to save the computational cost, the external environment model of the cab can be built by omitting the non-contact components and only retaining the steering wheel, seat and floor, which can be further appropriately simplified. The environment model is shown in Figure 4.

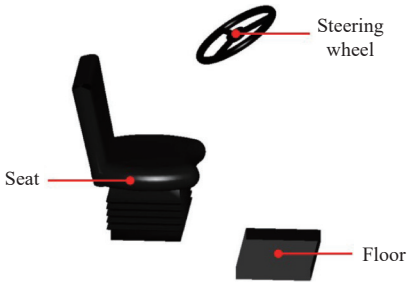

Figure 4 Environment model for steering wheel manipulation

2.1.3 Establishment of driver-steering wheel biomechanical coupling model

1) Settings of driver-steering wheel contact

To build the final coupled biomechanical model for the driver and steering wheel, it is necessary to couple the environment model for steering wheel manipulation with the musculoskeletal model and release the constraints. The voxels of the steering wheel, seat and floor were added to AnyBody, followed by the import of the model in STL format into these voxels and adjustment of the position. According to the literature, the hand and steering wheel were set as a spherical hinge connection, the lumbar back and backrest, the hip and seat cushion, and the foot and floor were set as linear contacts with friction coefficients of 0.22, 0.5, and 0.22, respectively[14,15].

When AnyBody is used to build a human model, some joints in the musculoskeletal model should be constrained in order to balance the degree of freedom. During the coupling process, the added connections will increase constraints on the human model. For a better balanced degree of freedom and free movement of the model, some internal joint constraints in the model should be released. The added constraints in this model are mainly caused by the connection between the arm and steering wheel. The spherical hinge connection of the left and right hands with the steering wheel will add three rotational constraints, respectively. Considering the movements of the arm joints when rotating the steering wheel, three internal joint constraints need to be released, including shoulder flexion and extension, shoulder external rotation and elbow flexion and extension[16]. In addition, as the human model in AnyBody is set as a rigid body with infinite strength, a direct connection between the hand and the steering wheel will generate an error report. Hence, an additional glove voxel needs to be added to the hand to confer the strength of the connection with a finite value, and transfer the force from the steering wheel to the glove and then to the hand. The biomechanical coupling model for tractor driver and the steering wheel is presented in Figure 5.

Figure 5 Driver-steering wheel biomechanical coupling model

2) Driving of the driver-steering wheel coupling model

AnyBody calculates the biomechanical properties of human musculoskeletal models primarily based on inverse dynamics analysis. Inverse dynamics first gives the structure with a motion mode, and then inversely calculates the force on the structure according to the laws of mechanics. Hence, correct driving of the model is important in the simulation. In the AnyBody simulation of steering wheel rotation, a torque is applied to the steering wheel, resulting in the rotation of the steering wheel and then the rotation of the arm in the musculoskeletal model. To simulate the process of steering wheel manipulation, this study used a torque detector to measure the torque of the steering wheel rotation in a ploughed field. The test tractor was a Dongfanghong LX804 wheel tractor, and the measurement was performed by fixing the detector to the steering wheel and collecting the torque when rotating the steering wheel for 90° while driving on ploughed field (Figure 6).

Figure 6 Torque measurement of the tractor steering wheel

According to the test results, the rotation angle of the steering wheel has a minor effect on the variation in torque when the driver rotates the wheel. The average torque for rotating the steering wheel on ploughed field reached 3 N·m, and therefore 3 N·m was selected as the torque input for the steering wheel in the simulation. In addition, to simulate the rotation process of the steering wheel, the rotation angle needs to be analyzed and set. In actual two-handed

operation, the angle of steering wheel rotation is generally no more than 90° in both the clockwise and counterclockwise directions, which is symmetrical in the degree of arm activation[17]. Therefore, to save the computational cost, the simulation was set up with a counterclockwise steering wheel rotation angle of 90°, a steering wheel torque of 3 N-m, a simulation time of 2 s, and a step length of 45 steps.

The main biomechanical indicator analyzed in the simulation is muscle activation level, which is the ratio of muscle force to the maximum muscle strength and can reflect the utilization rate of the muscle during exercise. In AnyBody, the muscle activation level is expressed as values ranging from 0 to 1, where 0 means that the muscle is not utilized, 1 indicates that the muscle is fully utilized, and a value above 1 represents that the muscle is overstressed and in a state of fatigue. In this state, the muscle is susceptible to strain and the muscle tissue is easily damaged[18]. To facilitate the subsequent validation of the simulation results using surface electromyography (sEMG) tests, the muscle activation level was converted to percentage when analyzing the simulation results, i.e. 0% to 100%.

3 Experiments

3.1 Verification of the driver-steering wheel coupling model

sEMG is a weak electrical signal collected on the surface of the human skin. It has the advantages of non-invasive and convenient operation, and is one of the most commonly used non-invasive muscle load measurement methods. sEMG is widely used in clinical medicine, sports science, ergonomics and research on muscle fatigue effects[19,20]. In this study, to verify the reliability of the biomechanical model, the sEMG signals of the driver's arm muscles were tested when rotating the steering wheel on a ploughed field, and the results were compared with those of simulation analysis.

3.1.1 Selection of muscles to be tested and calculation of maximum voluntary muscle contraction force

Since the sEMG signal is a weak electrical signal, and the electrical signal generated by the force of the deep muscles is transmitted to the skin surface, it will greatly weaken the signal and cause errors. Therefore, when selecting muscles for test, deep muscles should be avoided, and the superficial muscles beneath the skin should be selected. Therefore, in this study, the flexor carpi radialis, lateral head of triceps and biceps of the right arm were selected as the tested muscles.

The maximum voluntary muscle contraction force (maximum voluntary contraction, MVC) refers to the muscle contraction force when the length of muscle remains constant and the muscle tension reaches the maximum. Since the biomechanical index obtained by the simulation is the muscle activation degree, that is, the ratio of the muscle force to the maximum muscle strength, in the sEMG test, it is also necessary to measure the sEMG signal at the maximum MVC during the process of rotating the steering wheel of the tested muscle. The sEMG signal at the MVC force and finally the root mean square (RMS) value of the sEMG signal in the two states was calculated, respectively. The ratio of the two root mean square values is the muscle activation degree during the test. The specific formula for calculating the muscle activation degree is as follows.

$$MA = \frac{\mathrm{RMS}_{\mathrm{TEST}}}{\mathrm{RMS}_{\mathrm{MVC}}} \quad (1)$$

where, MA is the muscle activation degree, %; $\mathrm{RMS}_{\mathrm{TEST}}$ is the root mean square value of the sEMG signal of the muscle, μV; $\mathrm{RMS}_{\mathrm{MVC}}$ is the root mean square value of the sEMG signal of the muscle's MVC, μV.

3.1.2 sEMG testing instruments and methods

The sEMG signal acquisition device used for the test was the Cometa MiniWave, a wireless sEMG test system from Cometa, Italy, as shown in Figure 7.

Figure 7 sEMG signal test system

The subjects were three 50th percentile drivers, who had no upper limb joint and muscle disorders with good physical conditions during the test phase and had not exercised strenuously in 24 hours prior to the test. The sEMG signal was collected by buckling up an electrode patch onto the wireless sEMG sensor, which was then attached to the skin surface following the course of the muscle fibers. As the sEMG signal is weak and susceptible to interference from the test environment, the hair on the skin was cut off and the skin surface was wiped with 75% medical alcohol to clean up any stains and keratin on the skin surface. The attached wireless sEMG sensor is shown in Figure 8.

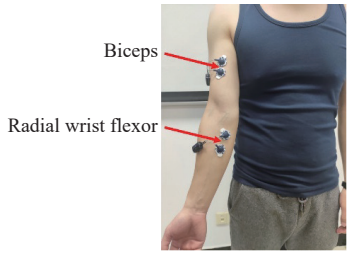

a. Biceps and radial wrist flexor

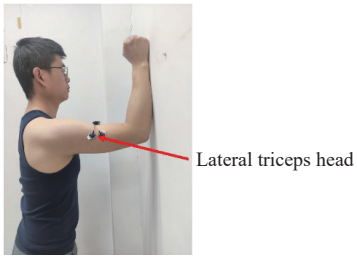

b. Lateral triceps head

Figure 8 Attachment of wireless surface electromyography sensor

After attachment of the wireless sEMG sensor, the first thing to do is to test the sEMG signal of the arm muscle at MVC force as follows.

(1) Radial wrist flexor: The subject is in a seated position with all four fingers except for the thumb placed together under the table, with an angle of 90° between the small arm and large arm. The subject primarily uses the four fingers to lift the table upwards, and the test worker ensures that the table is stable and immobile so that there is sufficient counterforce to stop the lifting up of the table.

(2) Biceps: The subject is in a seated position and places his entire palm under the table with an angle of 90° between the small arm and large arm. The subject uses the entire palm and the small arm to lift the table upwards, and the test worker ensures that the table is stable to prevent the table from being lifted upwards.

(3) Lateral triceps head: The subject assumes a standing position with his fist and arm resting against the wall at an angle of

90° between the small arm and large arm. The subject uses his fist and small arm to push forward against the wall, which gives sufficient counterforce to block the forward push.

The specific operations for the radial wrist flexors and biceps are shown in Figure 9 and those for the lateral head of the triceps are shown in Figure 8b. Once the subject had fully developed the force, the data were acquired. Each subject was tested three times for each muscle during the test, and each data acquisition lasted for three seconds. To prevent fatigue in the subject's arm, 5 min of rest was allowed between each test. After the test, the RMS values of the measured sEMG signals were calculated and the average of three tests for three subjects was taken as the final value.

a. Radial wrist flexor b. Biceps

Figure 9 Muscle MVC calibration action schematic

Once the sEMG signal at MVC force was tested, the real vehicle test could be carried out. After the sensor acquisition was switched on, the subject started to rotate the steering wheel for 90° counterclockwise on the ploughed field according to the simulation settings, and after the rotation was completed and held still, the sensor acquisition was terminated. The whole process lasted for five seconds and each subject was measured for three times. The RMS value of the measured sEMG signal was calculated after the test, and the average of three tests for three subjects was taken as the final value. The test site is shown in Figure 10.

Figure 10 sEMG signal test site

3.1.3 sEMG signal analysis and model validation

The sEMG signal is a non-smooth micro-electrical signal, which is susceptible to interference from other signals in the body such as ECG signals and industrial frequency noise during the acquisition process[21]. In addition, the sEMG signal is a low-frequency signal with an effective frequency range of 0-500 Hz and energy concentration of 20-150 Hz. Therefore, the sEMG signal needs to be pre-processed by offset removal, filtering and noise reduction. The purpose of offset removal is to adjust the initial position of the sEMG signal to zero potential; the low-pass and high-pass filters are both Butterworth filters with cut-off frequencies of 400 Hz and 10 Hz, respectively (as shown in Figure 11).

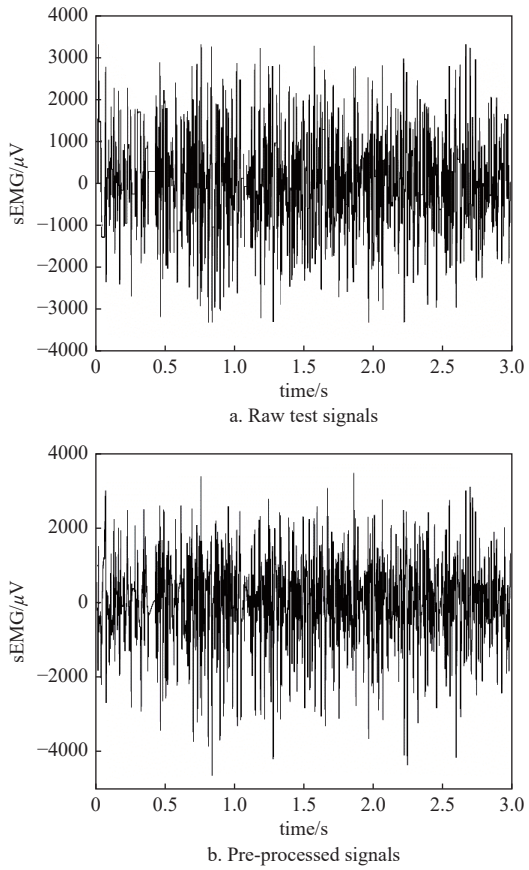

Figure 11 sEMG signal processing

For sEMG signals, RMS is mainly found in the time domain. The formula for calculating the RMS is as follows.

$$\mathrm{RMS} = \sqrt{\frac{1}{N}\sum x_i^2} \tag{2}$$

where, N is the number of points sampled in the test; and x_i is the amplitude at each sample point.

After obtaining the RMS value of the sEMG signal, the activation level of the arm muscles can be calculated according to Equation (1). Table 3 lists the activation levels of the radial wrist flexor, biceps brachii and lateral head of the triceps brachii muscles compared with the results of the simulation analysis.

Table 3 Comparison of muscle activation in test and simulation results

Tested muscles	Test/%	Simulation/%	Relative error
Radiocarpus	1.3620	1.4765	8.41%
Biceps brachii	0.4510	0.5003	10.93%
Triceps lateral head	0.3751	0.3288	12.34%

3.2 Analysis of muscle loading in the driver's arm based on the biomechanical model

3.2.1 Analysis and selection of muscles involved in arm activities

In the process of rotating the steering wheel, many muscles in the driver's arm are activated. However, some muscles do not change much during the operation process, and therefore the analysis should only involve the main muscle groups and muscles with high activation degrees during the rotation process. An

analysis of the driver's rotation of the steering wheel mainly involves the active joints of the shoulder, elbow and wrist[22], Therefore, deltoid, teres major, supraspinatus, subscapularis, brachialis, brachioradialis, biceps, lateral triceps head, pronator teres and radial wrist flexor were selected in this study. The muscle positions of the right hand are shown as an example in Figure 12.

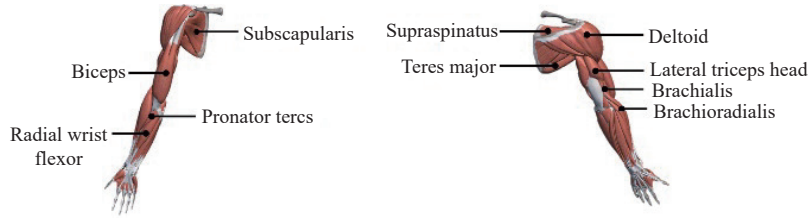

Figure 12 Position indication of each muscle

3.2.2 Analysis of the activation level of the driver's arm muscles during the rotation process

Based on the driver's biomechanical model, the arm system was analyzed in inverse dynamics by simulating the process of rotating the steering wheel at 90° counterclockwise and calculating the activation level of the main muscles in the left and right arms of each percentile driver.

As shown in Figure 13, during the 90° counterclockwise rotation of the steering wheel in each percentile, for the four main muscles involved in the shoulder joint activity, the activation degree gradually decreases on the left arm while tends to increase in the right arm with increasing rotation angle, and is always greater on the right arm than on the left arm. The main reason is that as the steering wheel rotates counterclockwise, the right arm will lift up, causing the shoulder joint to abduct, when the relevant muscles in the shoulder need to exert more force; however, the left arm drops down with the rotation of steering wheel, resulting in slow relaxation of the relevant muscles in the shoulder and gradual decreases of their activation levels till zero. In addition, among the related muscles on both arms, the deltoid muscle has the greatest muscle activation degree, indicating that this muscle exerts more force in the shoulder activity.

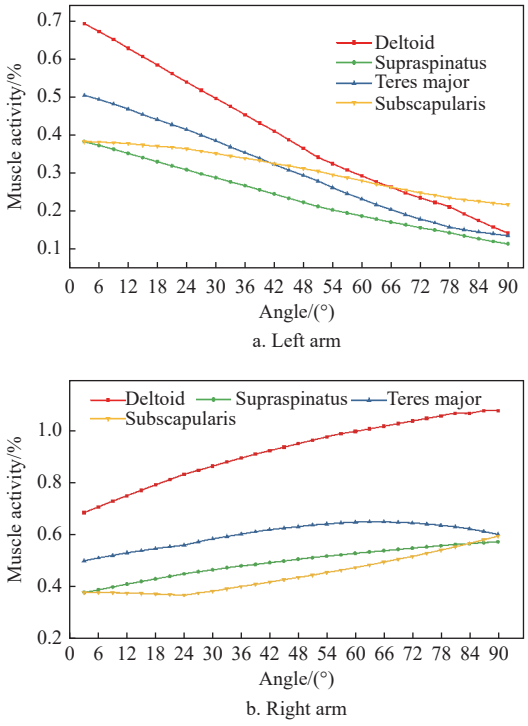

Figure 13 Activation of main muscles involved in shoulder joint of each percentile driver

As shown in Figure 14, during the 90° anticlockwise rotation of the steering wheel in each percentile driver model, among the main muscles involved in elbow joint activity, the activation of the brachioradialis muscle increases with increasing rotation angle on both the left and right arms; that of the lateral heads of the biceps and triceps decreases with decreasing angle; while that of the brachialis muscle decreases on the left arm and increases on the right arm with increasing angle. The activation of the brachialis muscle in the left arm decreases with increasing angle. Similar to the activation of the muscles for the shoulder joint, the activation of muscles associated with the elbow joint is also greater on the right arm than on the left arm. The reason is also likely that during the counterclockwise rotation of the steering wheel, the right arm elbow joint is raised upwards and the associated muscles need to exert more force, while the left arm elbow joint is gradually lowered and the associated muscles are gradually relaxed. In addition, the activation degree of the brachioradialis muscle is the greatest on both arms during the steering wheel rotation.

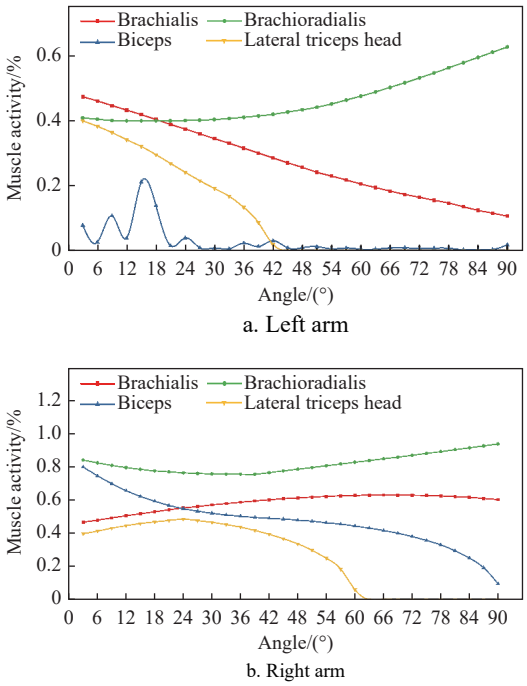

Figure 14 Activation of main muscles involved in elbow joint of each percentile driver

As demonstrated in Figure 15, during the 90° anticlockwise rotation of the steering wheel in each percentile driver model, the activation degrees of two muscles involved wrist joint increases on the left arm while first decreases and then increases on the right arm with increasing rotation angle. This is mainly because the left wrist

joint is gradually abducted and twisted outward with the rotation of the steering wheel. As the right wrist joint rotates inwards with the rotation of the steering wheel, the two muscles in the small arm are gradually relaxed accompanied by decreases in their activation. However, as the rotation angle increases, the small arm is lifted upwards with the steering wheel, making the muscles become tense, and therefore the activation of these two muscles in the small arm increases again with increasing rotation angle. Besides, in both arms, the activation of the pronator teres is always greater than that of the radial wrist flexor. In terms of the main muscles involved in different joint activities, the two muscles involved in wrist activity have significantly greater activation degrees than those muscles involved in elbow activities, indicating that the muscles involved in wrist activity are more active during the rotation process. Therefore, when optimizing the cab based on muscle activation levels, focus should be placed on reducing the activation degree of the two muscles involved in wrist joint activity.

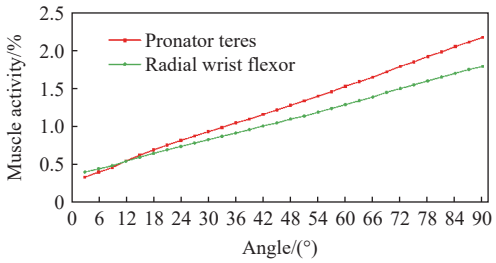

a. Left arm

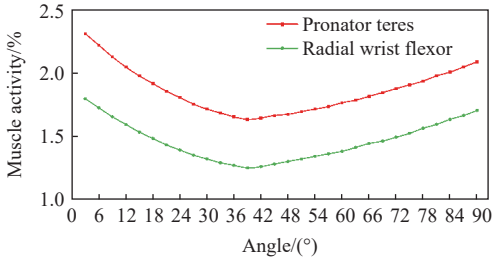

b. Right arm

Figure 15 Activation of main muscles involved in wrist joint of each percentile driver

3.2.3 Influence of steering wheel position parameters on muscle load of the driver's arm

1) Calculation of the integrated muscle activation of the driver' s arm

From the biomechanical simulation results, during the 90° counterclockwise rotation of the steering wheel, the right arm is raised upwards and has higher activation degrees of all muscles than the left arm. In the right arm, the pronator teres and radial wrist flexors involved in wrist movement have much greater activation degrees than the remaining muscles. In human arm muscle strength distribution, the large arm and shoulder have higher maximum muscle strength of muscles than the small arm[23]. In addition, the accumulation of muscle fatigue caused by frequent force on the pronator teres and radial wrist flexors can easily lead to muscle disorders such as pronator teres syndrome[24]. Therefore, the pronator teres and radial wrist flexors were taken to study the effect of tractor steering wheel position parameters on the degree of muscle activation. In order to unify the evaluation indicators and obtain the combined activation level of the two muscles, it is necessary to determine the weights of the influence of the two muscles. In this study, the coefficient of variation method was used to assign weights to the activation degree of the two muscles. The coefficient of variation was calculated using the following formula.

$$V_i = \frac{\sigma_i}{\bar{x}} (i = 1, 2, \cdots, n) \tag{3}$$

where, V_i is the coefficient of variation; σ_i is the standard deviation of the data; and $\bar{x}$ is the mean of the data. The coefficient of variation for the two muscles was calculated based on the standard deviation and mean of the muscle activation during the rotation of the steering wheel separately, and then the standard deviation was used to compare the mean. The formula for calculating the weights is as follows.

$$W_i = \frac{V_i}{\sum_{i=1}^{n} V_i} \tag{4}$$

where, W_i is the weight of each indicator; and V_i is the coefficient of variation. By using Equations (3) and (4), the weights W_1 and W_2 of the activation degree of the two muscles can be obtained, respectively, and then the RMS values of the activation degree of the two muscles during rotation can be found, which can be multiplied by the weights respectively and then summed to obtain the integrated muscle activation degree as follows.

$$MA_{COM} = W_1 MA_{PT} + W_2 MA_{FCR} \tag{5}$$

where, MA_{COM} is the combined muscle activation level; W_1 and W_2 are the weights of the anterior rotator circularis and radial wrist flexor, respectively; and MA_{PT} and MA_{FCR} are the root mean square values of the activation level of the anterior rotator circularis and radial wrist flexor, respectively.

2) Determination of steering wheel position parameters

The position parameters of the tractor steering wheel mainly include the steering wheel inclination angle θ, the front-back distance L and upper-lower height h from the steering wheel mid-point (W point) to the driver's hip point (H point). In the national standard GB/T 6235-2004, the seat size of agricultural tractors is specified, which sets a θ of 0°-40°, L of 425-525mm, and h of 265-385 mm. On this basis, five levels were selected for optimization analysis in this study by using the actual steering wheel measurement parameters as a benchmark. The factor levels for the steering wheel position parameters are listed in Table 4.

Table 4 Factor levels for steering wheel related parameters

Level	Factor		
	Inclination angle θ/(°)	Front-back distance L/mm	Upper-lower height h/mm
1	0	425	265
2	10	440	300
3	20	455	335
4	30	490	360
5	40	525	385

3) Effect of steering wheel position parameters on driver arm muscle loading

a. Effect of inclination angle on the degree of integrated muscle activation

By using the actual steering wheel measurement parameters as reference, the L in the model was set to 455 mm and h was set to 335 mm. Then, the degree of integrated muscle activation was simulated and analyzed at the inclination of 0°, 10°, 20°, 30° and 40°, respectively (Figure 16).

b. Influence of front-back distance on the degree of integrated muscle activation

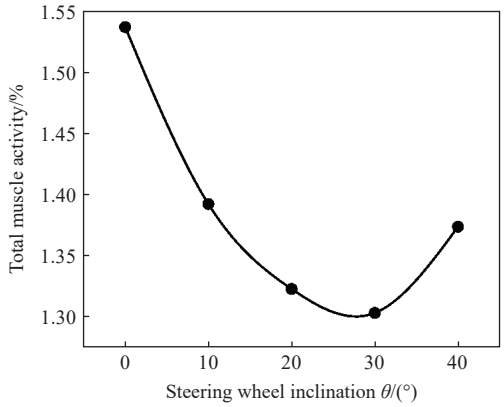

Figure 16 Effect of steering wheel inclination angle on integrated muscle activation

By taking the actual measurement parameters of the steering wheel as the benchmark, the h in the model was set to 335 mm, and θ was set to 40°. Then, the L was simulated and analyzed at 425 mm, 440 mm, 455 mm, 490 mm and 525 mm, and the change pattern of the integrated muscle activation degree with L could be obtained (Figure 17).

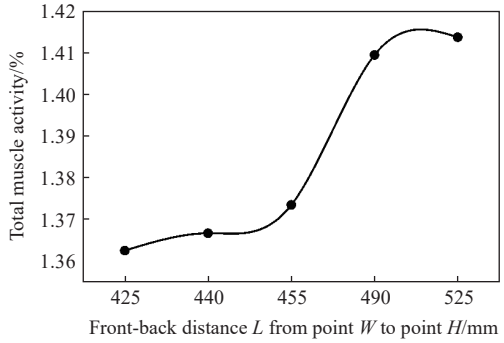

Figure 17 Effect of front-back distance on integrated muscle activation

c. Influence of upper-lower height on the degree of integrated muscle activation

By taking the actual steering wheel measurement parameters as a benchmark, the L was set to 455 mm, and the θ was set to 40°. Then, the h was simulated and analyzed at 265 mm, 300 mm, 335 mm, 360 mm and 385 mm. The change pattern of integrated muscle activation with h could be obtained (Figure 18).

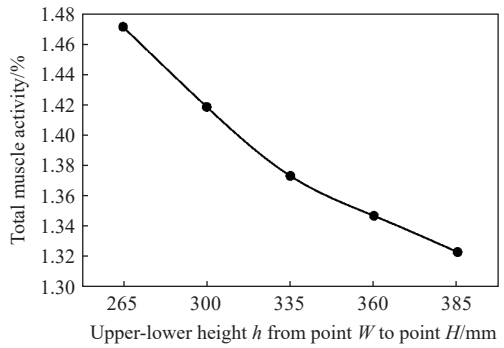

Figure 18 Effect of upper-lower height on integrated muscle activation

3.3 Optimization of tractor steering wheel position parameters

3.3.1 Response surface optimization design

Response surface methodology (RSM) is an optimization method proposed by Box and Wilson in 1995, which allows the optimal solution of a multivariate problem and finding of the optimal parameters after regression analysis. RSM has the advantages of a small number of tests, high accuracy and visualized results[25]. Response surface analysis is divided into two types of experimental design methods: BBD (Box-Behnken design) and CCD (central composite design), with the former being suitable for situations with a small number of factor levels, and the latter being suitable for multi-factor and multi-level experiments. With the same number of factor levels, BBD requires fewer times of test than CCD, and is therefore more convenient and efficient[26,27]. In this study, the number of factor levels in the optimization process was three factors and three levels. Hence, the BBD design was chosen for response surface analysis. The factors in the response surface simulation include steering wheel inclination angle θ, front-back distance L and upper-lower height h from point W to point H. Three levels were set for each factor, and the integrated muscle activation level was used as the response value in the response surface simulation. The factor levels for the response surface simulation of steering wheel position parameters are coded as listed in Table 5.

Table 5 Factor level coding for response surface simulation of steering wheel parameters

Level	Factor		
	A: Steering wheel inclination angle θ/(°)	B: Front-back distance/mm	C: Upper-lower height/mm
–1	20	425	335
0	30	440	360
1	40	455	385

After determination of the factor levels, a response surface simulation was carried out in AnyBody. The combination of factor levels and response values are listed in Table 6.

Table 6 Results of integrated muscle activation in combination of different factor levels

No.	A: Steering wheel inclination angle θ/(°)	B: Front-back distance/mm	C: Upper-lower height/mm	Y: Integrated muscle activation level
1	0	0	0	1.289 74
2	0	1	–1	1.303 04
3	0	0	0	1.289 77
4	–1	0	1	1.338 21
5	–1	1	0	1.324 39
6	1	0	1	1.314 33
7	1	–1	0	1.333 73
8	1	1	0	1.347 34
9	–1	–1	0	1.338 26
10	1	0	–1	1.366 75
11	–1	0	–1	1.319 82
12	0	–1	1	1.291 47
13	0	0	0	1.289 89
14	0	0	0	1.298 91
15	0	–1	–1	1.291 55
16	0	0	0	1.288 85
17	0	1	1	1.298 05

As shown in Table 6, there are certain differences between the integrated muscle activation degree under different combinations of factor levels. In order to achieve the optimization of the steering wheel position parameters, a regression model of the integrated muscle activation degree was established using the response surface method.

3.3.2 Development of the regression model for integrated muscle activation

Design-Expert 8.0 was used to carry out regression analysis of the simulation data for different combinations of steering wheel factor levels. Firstly, the integrated muscle activation level was fitted in a linear model, a two-factor interaction model and a second-order model, and the misfit terms p-value, R^2_{Adj} and R^2_{Pre} were obtained for the three models. The results are listed in Table 7.

Table 7 Fitting results of integrated muscle activation under different regression models

Model type	Linear	2FI	Second order
Misfit terms p-value	0.0007	0.0005	0.1707
R^2_{Adj}	–0.1736	–0.2842	0.9475
R^2_{Pre}	–0.7511	-2.1054	0.7390

As shown in Table 7, the second-order model has a p-value of 0.1707 for the misfit term among the three models, which is the most insignificant and the best fit. In addition, the R^2_{Adj} for the second-order model is 0.9475 and the R^2_{Pre} is 0.7390, both of which is close to 1, and the difference between R^2_{Adj} and R^2_{Pre} is close to 0.2. Therefore, the second-order model can provide an accurate fit for the integrated muscle activation level, and an ANOVA can be conducted on the second-order model for the integrated muscle activation level[28]. The ANOVA results are listed in Table 8.

Table 8 Analysis of variance of second-order regression model of integrated muscle activation

Source of variation	Sum of squares	Degree of freedom	Mean square	F-value	p-value	Significance
Model	9.37E-03	9	1.04E-03	33.10	< 0.0001	**
A	2.15E-04	1	2.15E-04	6.83	0.0347	*
B	3.97E-05	1	3.97E-05	1.26	0.2985	N
C	1.91E-04	1	1.91E-04	6.07	0.0432	*
AB	1.89E-04	1	1.89E-04	6.00	0.0442	*
AC	1.25E-03	1	1.25E-03	39.84	0.0004	**
BC	6.05E-06	1	6.05E-06	0.19	0.6742	N
A^2	7.30E-03	1	7.30E-03	231.94	< 0.0001	**
B^2	3.48E-05	1	3.48E-05	1.11	0.3279	N
C^2	1.25E-05	1	1.25E-05	0.40	0.5488	N
Residuals	2.20E-04	7	3.15E-05			
Misfit term	1.50E-04	3	4.99E-05	2.83	0.1707	N
Pure error	7.06E-05	4	1.76E-05			
Combined	9.59E-03	16				

Note: * indicates a significant effect (p<0.05); ** indicates a highly significant effect (p<0.01. A is the steering wheel inclination angle θ (°), B is the front-back distance L (mm), and C is the height h (mm) from point W to point H, and A^2, B^2 and C^2 represent the AA, BB and CC interactions.

As demonstrated in Table 8, the factors B, BC, B^2 and C^2 had no significant effect on the degree of integrated muscle activation (p>0.05), which were removed, and then the second-order regression model was refitted. Factor B was retained as it showed an effect on factor AB. An analysis of variance (ANOVA) was performed on the revised second-order regression model for the degree of integrated muscle activation and the results are listed in Table 9.

As shown in Table 9, the p-value of the model is lower than 0.0001, indicating that the second-order model is of a good fit. In addition, the coefficient of determination R^2 of the modified model is 0.9712, which is close to 1, and the R^2_{Pre} of the modified model is

Table 9 Analysis of variance of modified second-order regression model for integrated muscle activation

Source of variation	Sum of squares	Degrees of freedom	Mean square	F-value	p-value	Significance
Model	9.32E-03	6	1.55E-03	56.29	< 0.0001	**
A	2.15E-04	1	2.15E-04	7.79	0.0191	*
B	3.97E-05	1	3.97E-05	1.44	0.2582	N
C	1.91E-04	1	1.91E-04	6.93	0.0251	*
AB	1.89E-04	1	1.89E-04	6.84	0.0258	*
AC	1.25E-03	1	1.25E-03	45.43	< 0.0001	**
A^2	7.43E-03	1	7.43E-03	269.32	< 0.0001	**
Residuals	2.76E-04	10	2.76E-05			
Misfit term	2.05E-04	6	3.42E-05	1.94	0.2717	N
Pure error	7.06E-05	4	1.76E-05			
Combined	9.59E-03	16				

Note: * indicates a significant effect (p<0.05); ** indicates a highly significant effect (p<0.01). A is the steering wheel inclination angle θ (°); B is the front-back distance L (mm); and C is the height h (mm) from point W to point H, and A^2 represents the AA interaction.

0.9026, which is 22.14% higher than that before modification. The fitted function between the modified integrated muscle activation level and each factor is shown in the equation below.

$$Y = 1.29 + 5.18\times10^{-3}A + 2.23\times10^{-3}B - 4.89\times10^{-3}C + 6.67\times10^{-3}AB - 0.018AC + 0.042A^2 \quad (6)$$

where Y is the degree of integrated muscle activation; A is the steering wheel inclination angle θ (°); B is the front-back distance L, mm; and C is the height h from point W to point H, mm.

To determine the accuracy of the second-order regression model, this study plots the predicted values versus actual values of the integrated muscle activation degree and the residual distribution of the regression model on the basis of ANOVA (Figure 19).

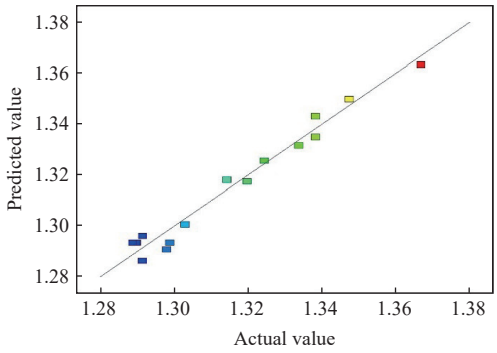

a. Comparison chart between predicted value and actual value

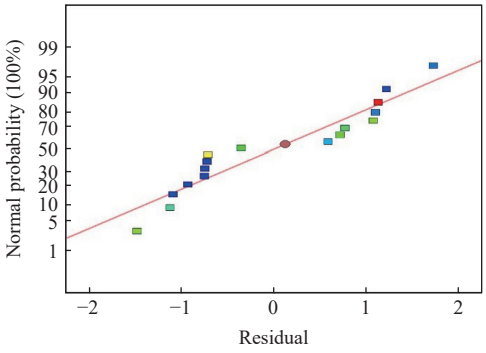

b. Residual distribution map

Figure 19 Comparison between predicted and actual values and residual distribution

As shown in Figure 19a, the predicted and actual values of the integrated muscle activation degree are almost distributed on the same line, indicating low error and high accuracy of the regression model prediction. Figure 19b shows that the residuals are generally distributed in a straight line, and the error between the predicted and actual values is small and follows a normal distribution, indicating a strong reliability of the fitted function. Therefore, it is possible to use Equation (6) to predict the degree of integrated muscle activation for different combinations of inclination angle, front-back distance and upper-lower height.

3.3.3 Influence of steering wheel position parameters on the degree of integrated muscle activation

Based on the ANOVA results, the contribution rate of each factor to the degree of integrated muscle activation can be calculated to compare the effect of each factor with the following equation[29].

$$\delta = \begin{cases} 0 & (F \le 1) \\ 1 - \dfrac{1}{F} & (F > 1) \end{cases} \tag{7}$$

where, F is the F-value of each factor in the ANOVA. The contribution of each factor can then be calculated as follows.

$$\Delta_j = \delta_j + \frac{1}{2} \sum_{\substack{i=1 \\ i \ne j}}^{m} \delta_{ij} + \delta_{jj} \tag{8}$$

where, Δ_j is the contribution of factor j; δ_j is the primary contribution of factor j; δ_{ij} is the contribution of factor ij interaction; and δ_{jj} is the secondary contribution of factor j. According to the F-value of each factor in Table 9, the contribution rate of each factor was calculated using Equations (7) and (8). As a result, the contribution rates of inclination angle, front-back distance and upper-lower height were calculated to be $\Delta A = 2.78$, $\Delta B = 0.73$ and $\Delta C = 1.34$, respectively. Therefore, the magnitude of influence of each factor on the degree of integrated muscle activation follows the order of inclination angle > upper-lower height > front-back distance. Furthermore, both the AB and AC interactions have significant effects on the degree of integrated muscle activation ($p<0.05$; Table 9). Hence, this study analyzes the pattern for the effect of factor interaction on integrated muscle activation degree based on the interaction response surface plot and contour plot.

1) Interactive effects of inclination angle and front-back distance on the degree of integrated muscle activation

The response surface plot for the interaction between steering wheel inclination (A) and front-back distance (B) is shown in Figure 20a. The contour plot of AB interaction is shown in Figure 20b, which can provide a more visual presentation of the effect of AB interaction on the degree of integrated muscle activation. It can be seen that the degree of integrated muscle activation is lower when the inclination angle is 25°-35° and the front-back distance is 432.5-447.5 mm.

2) Interactive effect of steering wheel inclination and upper-lower height on the degree of integrated muscle activation

The response surface plot for the interaction of steering wheel inclination (A) and upper-lower height (C) is shown in Figure 21a. Again, there is a minimum degree of integrated muscle activation for the AC interaction as shown in Figure 21b. The contour plot provides a more visual representation of the effect of AC interaction on the degree of integrated muscle activation. Overall, the degree of integrated muscle activation is lower when the inclination angle is 25°-35° and the upper-lower height is 347.5-372.5 mm.

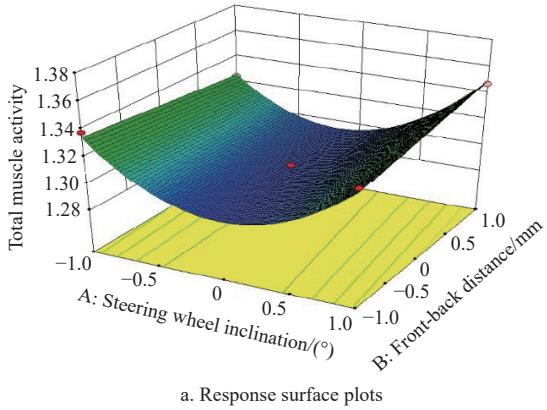

a. Response surface plots

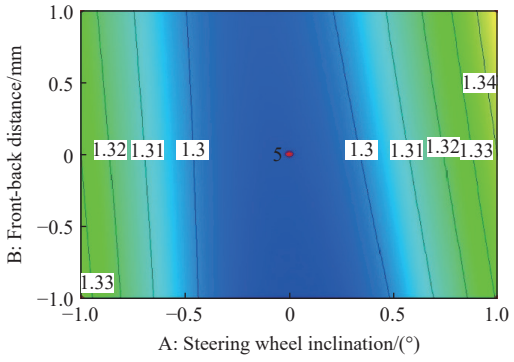

b. Contour plots

Figure 20 Response surface diagram and contour map of AB interaction

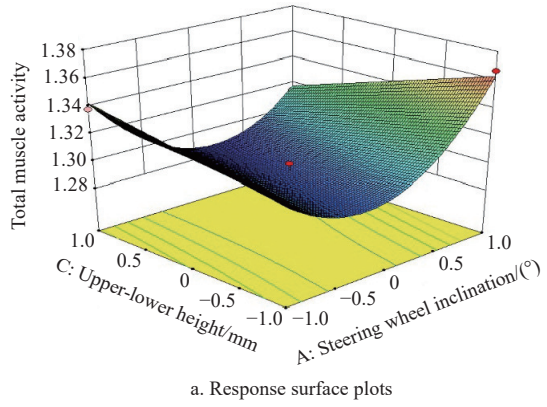

a. Response surface plots

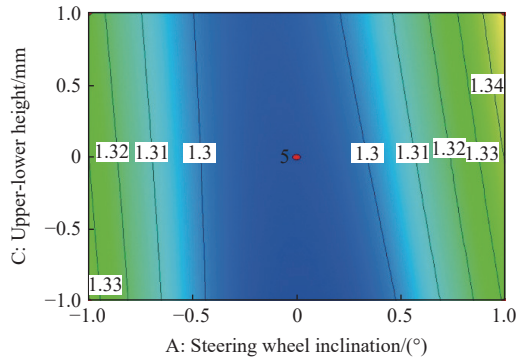

b. Contour plots

Figure 21 Response surface diagram and contour map of AC interaction

4 Discussion

In this study, the biomechanical modelling software AnyBody was used to carry out an inverse kinetic analysis of the tractor steering wheel twisting process, calculate the degree of muscle

activation in the driver's arm, and compare it with the results of sEMG tests on the same part of the arm. The analysis found that the relative error between the sEMG test results and the simulation analysis results ranged from 8.41% to 12.34%, These relative errors are caused by the inevitable test errors due to the influence of the position of the electrode pads and muscle superimposition, whereas the simulation analysis is based on inverse kinetics analysis, which can accurately calculate the activation level of each muscle. According to the literature, the acceptable range of relative error between the sEMG test and simulation analysis results should be lower than 15%[30]. Therefore, the biomechanical model established in this study has a high reliability.

By analysing the activation of the driver's arm muscles, it was found that the activation of the driver's right arm muscles was significantly greater than that of the left arm muscles during the counterclockwise twisting of the steering wheel, where the activation of the muscles involved in the wrist joint activity was much greater than that of the elbow and shoulder joints.

In order to reduce arm muscle fatigue during the frequent twisting of the steering wheel, the steering wheel position parameters of the tractor were optimized to determine the optimum combination of steering wheel position parameters. The test used three factors - steering wheel inclination, front-back distance and upper-lower height to investigate the effect of steering wheel position parameters on the degree of activation of the driver's integrated arm muscles, and the analysis found that with increasing inclination angle θ, the integrated muscle activation of the arm first decreases and then increases, reaching a minimum value at θ of 30°. The main reason for this is that at θ of 0°, the steering wheel is in a horizontal position and the wrist joint will bend greatly, causing the tightening of arm muscles and thus increasing the arm muscle activation degree. As θ increases, the flexion of the wrist joint gradually decreases and the muscles gradually relax, resulting in a gradual decrease in muscle activation. However, with further increases in θ, the rising distance of the right arm will become greater with the counterclockwise rotation, and when θ reaches a certain level, the muscle activation tends to increase again. In summary, to reduce the degree of integrated muscle activation, the optimal inclination angle θ is 30°, and the optimal range is 20°-40°. With increasing L, the integrated arm muscle activation gradually increases, and the increase is particularly significant when L changes from 455 to 490 mm. The reason is that when the L is small, the bending angles of the elbow and wrist joint movement angle are small during the rotation of the steering wheel. With increasing L, the angle of the elbow joint gradually increases, and the wrist joint needs a larger angle of circular movement during the rotation process, which together result in an increase in the degree of integrated muscle activation. Therefore, the optimum level of L is 425 mm, and the optimum range is 425-455 mm to reduce the degree of integrated muscle activation. The integrated activation degree of the arm muscles gradually decreases with increasing H. The reason is that when h is small, the angle of the elbow joint is large, and the wrist joint will have a larger angle of circular rotation when rotating the steering wheel; while as h increases, the angle of the elbow joint decreases, and the circular rotation angle of the wrist joint will gradually decrease when rotating the steering wheel, resulting in a gradual decrease in the degree of integrated muscle activation. Therefore, the optimum level of h is 385 mm, with an optimum range of 335–385 mm to reduce the overall muscle activation.

Based on the above analysis, the three steering wheel position parameters were optimized using the second-order regression model with the lowest integrated muscle activation level as the target, and the optimization results were verified by simulation. The optimum combination of the position parameters is coded as $A = 0.1$, $B = –0.6$ and $C = 0.6$ after response surface analysis, i.e. an inclination angle θ of 31°, a front-back distance L of 431 mm and an upper-lower height h of 375 mm. Under this combination, the value of the integrated muscle activation level was predicted to be 1.2887. In order to verify the reliability of the optimization results, the biomechanical model was used as the test platform for simulation and analysis at the θ of 31°, L of 431 mm and h of 375 mm.

5 Conclusions

This study aims to analyze the changes in arm muscle activation during the driver's rotation of the tractor steering wheel, investigate the effect of steering wheel position parameters on arm muscle activation, and finally determine the optimal position parameters for the steering wheel. AnyBody was first used to carry out an inverse kinetics analysis of the tractor steering wheel rotation process and calculate the activation level of the driver's arm muscles. Based on the biomechanical model, the effects of three position parameters (steering wheel inclination angle, front-back distance and upper-lower height) on the activation degree of the driver's arm muscles were then analyzed. The results show that the steering wheel inclination angle has the most significant effect on the degree of overall muscle activation, followed by the upper-lower height and then the front-back distance. Taking into account the interaction between factors, a regression orthogonal test revealed that the activation of the driver's arm is the minimum (1.2887) at the inclination angle of 31°, front-back distance of 431 mm and upper-lower height of 375 mm. This study optimizes the tractor steering wheel position parameters from the biomechanical point of view to reduce the fatigue of the driver's arm, but does not consider the influence of steering wheel position parameters on other biomechanical characteristics such as joint forces or moments, which needs to be addressed in further studies.

Acknowledgements

This work was financially supported by National Natural Science Foundation of China (Grant No. 51875230, 52175232).

[References]

[1] Hruška M. Assessment of the actual hand position on the steering wheel for drivers of passenger cars while driving. Agronomy Research, 2018; 16(4): 1668–1676.

[2] Yang Y, Li W J, Li Y K, Xu L Y, Wang Y P, Chen L Q. Ergonomics design of tractor clutch pedal based on biomechanical model. Transactions of the CSAE, 2019; 35(3): 82–91.

[3] Gopalrao M C, Niteen S, Shatrunjoy B, Shekhar P. Improved clutch pedal ergonomic position through adjustable clutch pedal assembly as per anthropometry. 16th Symposium on International Automotive Technology. Sage CA: Maharashtra CA: SAGE Publications.

[4] Feyzi M, Navid H, Dianat I. Ergonomically based design of tractor control tools. International Journal of Industrial Ergonomics, 2019; 72: 298–307.

[5] Qin Z Z, Shang Y J, Jiang W, Li H, Xu H M, Zhang G Z. Comfort evaluation and position parameter optimization of the clutch pedal in agricultural machinery based on a multi-level evaluation index system. Transactions of the ASABE, 2021; 64(6): 1805–1816.

[6] Jin X Q, Zhang J Y, Liu Y H. The ergonomics research of the joystick in excavator cab. Applied Mechanics & Materials, 2014; 494-495: 128–131.

[7] Zhang W J, Wang Q C, Xu Z, Shang Y J, Xu H M. Development of a tractor operator-operation environment coupled biomechanical model and analysis of lower limb muscle fatigue. Journal of Industrial Ergonomics, 2023; 93: 103407.

[8] Jiang W. Comfort evaluation and optimization of position parameters of agricultural machinery cab operating device. Huazhong Agricultural University, Wuhan, China. 2020. (in Chinese)
[9] Chen L, Li W, Yang Y, Miao W. Evaluation and optimization of vehicle pedal comfort based on biomechanics. Proceedings of the Institution of Mechanical Engineers, 2020; 234(5): 1402–1412.
[10] Liu S P, Si W, Yan Z Z, Xu C W. The human motions modeling and simulation based on anybody technology. Progress in Biomedical Engineering, 2010; 31(3): 131–134.
[11] Lee S, Park J, Jung K. Development of statistical models for predicting a driver's hip and eye locations. Proceedings of the Human Factors and Ergonomics Society Annual Meeting. Sage CA: Los Angeles, CA: SAGE Publications, 2017; 61(1): 501–504.
[12] Li W H, Zhang M, Lv G M, Han Q Y, Gao Y J, Wang Y, et al. Biomechanical response of the musculoskeletal system to whole body vibration using a seated driver model. International Journal of Industrial Ergonomics, 2015; 45: 91–97.
[13] Li H T, Qiao M M. Research on the mechanism of elbow flexion based on AnyBody, ICAPC, 2020; 1650: 022088.
[14] Gao F. Study of driver's fatigue mechanism and driving comfort evaluation based on musculoskeletal biomechanics. Jilin University, Changchun, China. 2017. (in Chinese)
[15] Wang X Y. Human-machine interaction design of vehicle control components considering the musculoskeletal characteristics. Jilin University, Changchun, China. 2020. (in Chinese)
[16] Li M Y. Research on vehicle seat sitting comfort based on passengers' pressure distribution and physiologic information. Jilin University, Changchun, China. 2020. (in Chinese)
[17] Wang H Y. Driving comfort based on the simulation and analysis of muscle force. Hefei University of Technology, Hefei, China. 2016. (in Chinese)
[18] Ding C, Wang J Z, Gao Z. Inverse dynamics simulation of the musculoskeletal model of human legs in driving based on AnyBody modeling system. Chinese Journal of Biomedical Engineering, 2013; 32(1): 124–128. (in Chinese)
[19] Meng Q F, Tao Q, Lai Q B, Hu Y G. Study on the performance of elbow muscle fatigue assessment using SEMG. Machinery Design & Manufacture, 2023; 3: 53–57, 62. (in Chinese)
[20] Xu Z, Lu J, Pan W J, He K L. Fatigue analysis of upper limb rehabilitation based on surface electromyography signal and motion capture. Journal of Biomedical Engineering, 2022; 39(1): 92–102.
[21] Somar K, Ali M, Jean B C, Djaffar O A. sEMG time-frequency features for hand movements classification. Expert Systems with Applications, 2022; 210: 118282.
[22] Gao Z H, Fan D, Wang D P, Cheng Y, Wang Y H. Mechanical characteristics simulation of driver's upperlimb muscles in steering maneuver. Automotive Engineering, 2016; 38(1): 47–52.
[23] Yu H J. Development of a high-fidelity human muscle fatigue model with physiological characteristics for use in the modeling of the elbow flexor-extensor motion. Fudan University, Shanghai, China. 2008. (in Chinese)
[24] Rasmussen M B, Deutch S R. Pronator teres syndrome is a rare but important cause of pain in the forearm. Ugeskrift for laeger, 2016; 178 (46): 30977697.
[25] Liu Q J, Luo X W, Zeng S, Zang Y, Wen Z Q, Zeng L, et al. Numerical simulation and experiment of grain motion in the conveying system of ratooning rice harvesting machine. Int J Agric & Biol Eng, 2022; 15(4): 103–115.
[26] Azad F N, Ghaedi M, Asfaram A. Optimization of the process parameters for the adsorption of ternary dyes by Ni doped FeO (OH)-NWs–AC using response surface methodology and an artificial neural network. RSC advances, 2016; 6(24): 19768–19779.
[27] Yolmeh M, Jafari S M. Applications of response surface methodology in the food industry processes. Food and Bioprocess Technology, 2017; 10(3): 413–433.
[28] Wang Q C, Shang Y J, Qin Z Z, Xu H M, Jiang W, Li H, et al. Comfort evaluation and position parameter optimization of the steering wheel in agricultural machinery based on a three-level evaluation index system. Int J Agric & Biol Eng, 2022; 15(4): 214–222.
[29] Wei Jiang, Jie Zhou, Hongmei Xu, Shuang Liu, Chenglong Wang, Jiajun Dong. Research of the Influence of Road Excitation on Human Body Comfort under the Harvester Working Condition. Applied Engineering in Agriculture, 2019; 35(4): 495–502
[30] Gao F, Zong S, Han Z W, Xiao Y, Gao Z H. Musculoskeletal computational analysis on muscle mechanical characteristics of drivers' lumbar vertebras and legs in different sitting postures. Revista Da Associacao Medica Brasileira, 2020; 66(5): 637–642.